FFEMS Fatigue & Fracture of Engineering Materials & Structures

doi: 10.1111/ffe.12241

A convenient way to represent fatigue crack growth in structural adhesives

R. JONES[1], W. HU[1] and A. J. KINLOCH[2]

[1]*Centre of Expertise for Structural Mechanics, Department of Mechanical and Aerospace Engineering, Monash University, Clayton, Victoria, 3800, Australia,* [2]*Department of Mechanical Engineering, Imperial College London, Exhibition Road, London SW7 2AZ, UK*

Received Date: 27 April 2014; Accepted Date: 1 August 2014; Published Online: 2014

ABSTRACT The present paper examines crack growth in a range of aerospace and automotive structural adhesive joints under cyclic-fatigue loadings. It is shown that cyclic-fatigue crack growth in such materials can be represented by a form of the Hartman–Schijve crack-growth equation, which aims to give a unique and linear 'master' representation for the fatigue data points that have been experimentally obtained, as well as enabling the basic fatigue relationship to be readily computed. This relationship is shown to capture the experimental data representing the effects of test conditions, such as *R*-ratio and test temperature. It also captures the typical scatter often seen in the fatigue crack-growth tests, especially at low values of the fatigue crack-growth rate. The methodology is also shown to be applicable to both Mode I (opening tensile), Mode II (in-plane shear) and Mixed-Mode I/II fatigue loadings. Indeed, it has been demonstrated that the fatigue behaviour of structural adhesives under both Mode I and Mode II loadings may be described by one unique 'master' linear relationship via the Hartman–Schijve approach.

Keywords adhesives; fatigue crack growth; Hartman–Schijve equation; joints; mode mix; safe life.

NOMENCLATURE

a = crack length
A = a constant in the Hartman–Schijve equation
da/dN = rate of crack growth per cycle
D = a constant in the Hartman–Schijve crack-growth equation
G = strain-energy release rate
G_c = quasi-static value of the fracture energy
G_{max} = maximum value of the applied strain-energy release rate in the fatigue cycle
G_{min} = minimum value of the applied strain-energy release rate in the fatigue cycle
ΔG = range of the applied strain-energy release rate in the fatigue cycle, as defined later
$\Delta G_I = G_{Imax} - G_{Imin}$
$\Delta\sqrt{G_I}$ = range of the applied strain-energy release rate in the fatigue cycle, as defined later
$\Delta\sqrt{G_I} = \sqrt{G_{Imax}} - \sqrt{G_{Imin}}$
$\Delta\sqrt{G_{Ith}}$ = value of $\Delta\sqrt{G_I}$ at a value of da/dN of 10^{-10} m cycle^{-1}
$\Delta\sqrt{G_{Itbr}}$ = range of the fatigue threshold value of $\Delta\sqrt{G_I}$, as defined later.
$\Delta\sqrt{G_{Itbr}} = \sqrt{G_{Itbr.max}} - \sqrt{G_{Itbr.min}}$
Δk = crack driving force; see Eq. (2)
K = stress-intensity factor
K_{max} = maximum value of the applied stress-intensity factor in the fatigue cycle
K_{min} = minimum value of the applied stress-intensity factor in the fatigue cycle
ΔK = range of the applied stress-intensity factor in the fatigue cycle, as defined later
$\Delta K = K_{max} - K_{min}$

Correspondence to: R. Jones and A. J. Kinloch. E-mail: rhys.jones@monash.edu; a.kinloch@imperial.ac.uk

ΔK_{thr} = range of the fatigue threshold value of the applied stress-intensity factor, as defined later
$\Delta K_{thr} = K_{thr.max} - K_{thr.min}$
m = exponent in the Paris crack-growth equation
n = exponent in the Hartman–Schijve crack-growth equation
N = number of fatigue cycles
R = displacement ratio ($=\delta_{min}/\delta_{max}$)
R^2 = the linear correlation coefficient
α = a constant
β = a constant
δ_{max} = maximum displacement applied during the fatigue test
δ_{min} = minimum displacement applied during the fatigue test
I, II = subscripts indicating Mode I (opening tensile) and Mode II (in-plane shear) loads

INTRODUCTION

Adhesively bonded components and bonded repairs are widely used throughout the aerospace industry. However, given the central role that damage-tolerance assessment and analysis play in the design and certification of modern aerospace structures and bonded repairs,[1] it is imperative to understand their cyclic-fatigue behaviour. Further, it is important to have a sound, and validated, means for accounting for the effects of test conditions, such as *R*-ratio, test temperature and type of loading, and the inherent variability, and hence scatter, seen in the fatigue performance of structural adhesives. In this context, it should be noted that recent papers, for example, Pascoe *et al.*[2] and Azari *et al.*,[3] have provided an excellent review of the methods available for predicting fatigue crack growth in both adhesively bonded components and polymeric-matrix fibre composites.* The measurement and predictive methods developed so far, for example, Pascoe *et al.*,[2] Azari *et al.*,[3] Ripling *et al.*,[5] Jethwa and Kinloch[6] and Curley *et al.*,[7] have been largely based upon the principles of linear-elastic fracture mechanics (LEFM). Nevertheless, the use of fracture-mechanics methods for design and life-prediction studies for structural adhesives still represents relatively new areas of research and has yet to be adopted by design engineers.

Current fracture-mechanics approaches to crack growth in structural adhesive joints (and also in the polymeric matrix in fibre-composite materials, as discussed later) are based on variants of the Paris crack-growth equation, where the rate of crack growth per cycle, da/dN, is assumed to be linearly related to either $(G_{max})^m$ or $(\Delta G)^m$. Here, G_{max} is the maximum value of the applied strain-energy release rate in the fatigue cycle, and ΔG is the range of the applied strain-energy release rate in the fatigue cycle; see Eq. (5). However, several major problems have been found to arise with this approach. Firstly, unfortunately, the value of the exponent, m, in this relationship tends to be relatively large for structural adhesives (and fibre-composite materials). Secondly, fatigue crack growth may be initiated from relatively small naturally occurring material discontinuities and be more rapid than predicted from experimental data obtained from relatively 'long-crack' tests. Thirdly, how to account for typical scatter that is observed in the experimental fatigue tests is a challenge. Fourthly, how to account for, and model, the effects of the particular test conditions, such as the *R*-ratio employed, the test temperature and the mode of loading, has yet to be resolved.

The present paper represents the first paper to study the use of the Hartman–Schijve approach to model fatigue crack growth in structural adhesives and so hopefully offer a solution to such major design and life-prediction problems when employing structural adhesive bonding in aerospace applications. The first step in investigating whether this approach can be used for predicting debond growth in adhesives is to establish whether this approach can be used to represent the crack growth reported in experimental test data taken from the existing literature on 'long cracks' in structural adhesive joints, where the crack is propagating through the adhesive layer.

The value of the exponent

As commented earlier, in the Paris crack-growth equation, the rate of crack growth per cycle, da/dN, is assumed to be linearly related to either $(G_{max})^m$ or $(\Delta G)^m$ where the exponent m is a constant that is determined experimentally. Unfortunately, for structural adhesives and fibre-composite materials, the value of the exponent, m, in this relationship tends to be relatively large, for example,

*Whilst international test standards[4] do exist for linear-elastic fracture-mechanics testing of structural adhesives at quasi-static rates, none exist for cyclic-fatigue crack-growth tests.

Azari *et al.*,[3] Ripling *et al.*,[5] Jethwa and Kinloch[6] and Curley *et al.*,[7] Mall *et al.*,[8] Pirondi and Nicoletto[9] and Martin and Murri.[10] As a result, Martin and Murri[10] and Jones *et al.*[11] concluded:

> For composites, the exponents for relating propagation rate to strain-energy release rate have been shown to be high especially in Mode I. With large exponents, small uncertainties in the applied loads will lead to large uncertainties (of at least one order of magnitude) in the predicted delamination growth rate. This makes the derived power-law relationships unsuitable for design purposes.

The same situation holds for fatigue crack growth in structural adhesives. This can be seen in Fig. 1 where we present the da/dN versus G_{Imax} relationship obtained by Kinloch *et al.*[12] for a series of (nominally identical) tests on a typical rubber-toughened epoxy-film adhesive ('EA9628' from Hysol, USA) that is used widely in aerospace applications, where the subscript '*I*' indicates Mode I loading. In this instance, the exponent, m, varies from 7.97 to 6.92. Now, G is related to K^2, where K is the stress-intensity factor. Thus, if the relationship were to be expressed in terms of K_{max}, this corresponds to da/dN being proportional to $(K_{max})^{15.94}$ and $(K_{max})^{13.84}$, respectively. Thus, as noted earlier, this makes the derived power-law relationships unsuitable for design purposes.

This shortcoming has led to the aerospace industry adopting a 'no-growth' design philosophy for adhesively bonded components and composite structures; that is, designs are such that there would be no debond or delamination crack growth allowed during the lifetime of the aircraft.[13]

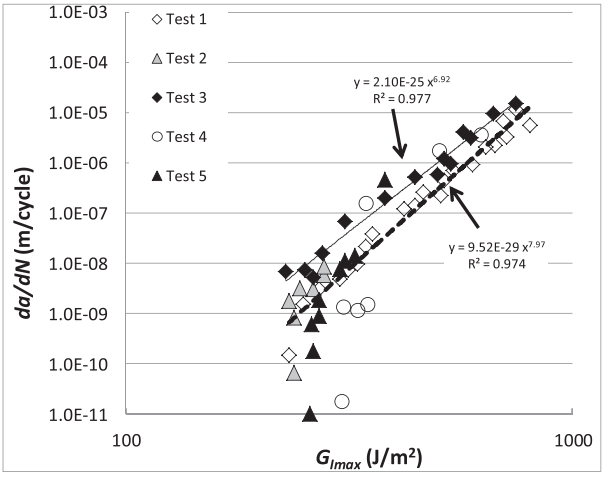

Fig. 1 The measured[12] Mode I fatigue behaviour for the rubber-toughened epoxy-film adhesive (Hysol 'EA9628').

Fatigue crack growth from 'small cracks'

Notwithstanding the previous statement, Jones *et al.*[14] has presented a number of examples, viz: in the 'F-111', 'A-320', 'F/A-18' and Canadian 'CF-5' aircraft, where fleet data and data obtained from full-scale fatigue tests[13] revealed that small sub-millimetre initial delaminations or debonds can grow when subjected to operational flight loads. As such, the inability of the 'no-growth' design approach to ensure that there is no in-service debond or delamination crack growth has led to the realisation that there is a need to allow for some slow crack growth in the initial design and thereby determine the appropriate inspection intervals. This approach to certifying adhesively bonded and composite structures was introduced in the 2009 US Federal Aviation Administration Airworthiness Advisory Circular.[15] It is hypothesised that this approach to certifying adhesively bonded and composite structures may be possible if it is possible to develop a crack-growth equation where the exponent is similar to that seen in metals.

To manage the growth of debonds and delaminations in operational aircraft, it is necessary to be able to account for the growth of such debonds or delaminations from small naturally occurring material discontinuities. In such instances, Jones[16] revealed that, for metals, it is essential to use a da/dN versus ΔG curve that represents growth from such naturally occurring material discontinuities. Therefore, the present challenge is how to determine a representation with a small exponent that has the potential of assessing sustainment problems associated with such small naturally occurring debonds and delaminations. It is well known that, for metals, experimental da/dN versus ΔK data obtained from American Society for Testing and Materials (ASTM) standard tests on 'long cracks' should not be used for assessing the growth of small naturally occurring cracks.[16] However, a strength of the Hartman–Schijve approach[16,17] is that, for metals, it can be used to determine the appropriate 'small cracks' relationship from such 'long-crack' test data, as well as accounting for other aspects of fatigue test data such as the effect of the R-ratio on the crack-growth rate and the scatter that is frequently observed in the data especially at low values of crack-growth rate, as discussed in detail later.

Scatter in the fatigue crack-growth data

One of the phenomena seen in the growth of small naturally occurring cracks in metallic airframes under representative operational loading is the relatively large scatter observed in the crack depth versus flight hours relationships.[16] However, as explained by Jones,[16] one of the advantages of the Hartman–Schijve approach is that this scatter can be captured by allowing for the variability

in both the size of the initiating material discontinuity and the fatigue threshold term in the Hartman–Schijve equation. It has also been shown[16] that, when the initial crack length was held constant, the variability in the resultant crack length versus cycles hours could be captured by allowing the fatigue threshold term to vary.

For crack growth in metallic airframes, the life and inspection intervals are determined by the fastest growing cracks, which[18] refers to as 'lead cracks'. In such cases, Wanhill[19] stated that 'it appears that fatigue crack growth thresholds are largely irrelevant for short/small → long/large fatigue crack growth'. In operational aircraft, where cracking generally starts from small naturally occurring material discontinuities, it therefore follows that the threshold term in the Hartman–Schijve equation is very small. As such, when assessing the variability in the life associated with lead cracks that grow from small naturally occurring material discontinuities in operational aircraft, the effect of the variability in the threshold term can essentially be ignored, and the scatter in the lives can be described by the probability distribution associated with the size of the initiating defect.[20] It is currently unclear if a similar approach could be used to assess the scatter seen in crack growth associated with adhesively bonded structures.

Current overall aims

Therefore, from the previous comments and observations, the present paper represents a first step to study whether cyclic-fatigue crack growth in structural adhesive joints can be represented by a form of the Hartman–Schijve crack-growth equation. Particular attention is given to whether

- The experimental fatigue crack-growth data may be represented by the Hartman–Schijve equation using a relatively low value for the threshold term with an exponent in the range of 2 to 3.
- The variability, and hence scatter, seen in the fatigue crack growth in the adhesive joints analysed in this paper can be represented using the Hartman–Schijve equation by allowing for variations in the associated threshold term.
- The Hartman–Schijve approach will allow a convenient reconciliation of the effects of the test conditions, such as the *R*-ratio, test temperature and mode of loading.

However, in connection with the scatter associated with fatigue crack-growth tests, it should be stressed that the 'metals' approach may well have to be extended so as to allow for scatter due to other sources, for example, surface treatment procedures when interfacial crack growth is recorded, that do not arise in the case of metallic airframes. It is also noteworthy that 'short cracks' effects, and the scatter associated with the growth of such naturally occurring defects, in structural adhesives may indeed be of importance when assessing the operational performance of adhesively bonded aircraft structures. Since, whilst there are currently no laboratory tests on the growth of small cracks in adhesives, the experience with the growth of small sub-millimetre initial debonds in the 'F-111' doubler and the 'F/A-18' titanium stepped lap joint subjected to operational load spectra,[16] as discussed earlier, does suggest the existence of 'short-crack' effects in adhesively bonded joints under operational load spectra. These aspects will be the subject of a subsequent paper.

THEORETICAL BACKGROUND

A recent state-of-the-art review of the field of fatigue crack growth and damage tolerance[16] has revealed that, in metals, the effects of changing the *R*-ratio and the growth of both 'long cracks' and 'short cracks', which grow from small naturally occurring material discontinuities, may be modelled using a form of the Hartman–Schijve crack-growth equation. This approach aims to give a unique and linear representation for the fatigue relationships that have been experimentally obtained. In principle, such a unique, that is, 'master' linear representation of the fatigue data should account for *R*-ratio and 'short-crack' effects and, thus, be of great assistance to a designer who wishes to predict the rate of crack growth in an adhesively bonded component. The Hartman–Schijve[11,14,16,17] equation is basically an empirical equation of the form:

$$\frac{da}{dN} = \beta(\Delta k)^{\alpha} \tag{1}$$

where β and α are constants, da/dN is the increment in the crack length per cycle and the 'crack driving force', Δk, is taken to be

$$\Delta k = \frac{(\Delta K - \Delta K_{thr})}{\sqrt{\{1 - K_{max}/A_1\}}} \tag{2}$$

where A_1 is a constant and ΔK is the range of the applied stress-intensity factor such that

$$\Delta K = K_{max} - K_{min} \tag{3}$$

and

$$\Delta K_{thr} = K_{thr.max} - K_{thr.min} \tag{4}$$

where K_{max} and the K_{min} are the maximum and minimum values of the applied stress-intensity factor in a fatigue

cycle, respectively, and the subscript '*thr*' in Eqs (2) and (4) refers to the threshold value, such that ΔK_{thr} represents the range of the fatigue threshold value. (Below the threshold value, ΔK_{thr}, no significant fatigue crack growth is considered to occur.)

It is well established[21,22] that for cracks in a thin layer of polymeric adhesive sandwiched between two relatively rigid composite or metallic substrates, the region that is dominated by the $r^{-1/2}$ singularity in the stress field, where r is the distance ahead of the crack, is exceptionally small. As a result, the strain-energy release-rate, G, approach, and not the stress-intensity factor approach, is generally used when employing a fracture-mechanics approach to investigate the failure of structural adhesives.[22,23] At first sight, the most obvious and corresponding parameter against which to plot the rate of fatigue crack growth, da/dN, is the range of applied strain-energy release rate, ΔG_I, such that

$$\Delta G_I = G_{Imax} - G_{Imin} \tag{5}$$

where G_{Imax} and the G_{Imin} are the maximum and minimum values of the applied strain-energy release rate in a fatigue cycle, respectively, and the subscript '*I*' refers to the opening, tensile mode of fracture. However, it is noteworthy that, for structural adhesives, many authors, for example, Jethwa and Kinloch[6] and Curley *et al.*,[7] have selected the parameter, G_{Imax}, rather than ΔG_I, to employ when analysing the fatigue behaviour. This is on the grounds that, during the unloading part of the fatigue cycle, the debonded surfaces typically come into contact, which results in facial interference of the adhesive surfaces, and the belief that this may give an artificially high value of G_{min}.[10] Notwithstanding, other authors[8] have shown that G_{Imax} approaches may lead, somewhat misleadingly, to an apparent strong dependence of the measured fatigue behaviour upon the R-ratio employed.

More recently, work has shown[11,14,24] that, to describe the cyclic-fatigue behaviour of adhesive joints and polymeric fibre composites, the term $\Delta\sqrt{G_I}$ should be employed, because $\Delta\sqrt{G_I}$ is directly equivalent to Eq. (3), which has some physical justification.[25] Thus, the form of the Hartman–Schijve equation† now becomes

$$\frac{da}{dN} = D\left[\frac{\Delta\sqrt{G_I} - \Delta\sqrt{G_{Ithr}}}{\sqrt{\left\{1 - \sqrt{G_{Imax}}/\sqrt{A}\right\}}}\right]^n \tag{6}$$

where D, n and A are constants and where the term $\Delta\sqrt{G_I}$ is defined by

$$\Delta\sqrt{G_I} = \sqrt{G_{Imax}} - \sqrt{G_{Imin}} \tag{7}$$

to give

$$\Delta\sqrt{G_{Ithr}} = \sqrt{G_{Ithr.max}} - \sqrt{G_{Ithr.min}} \tag{8}$$

and the subscript '*thr*' in Eqs (6) and (8) refers to the values at threshold, such that $\Delta\sqrt{G_{Ithr}}$ represents the range of the fatigue threshold value as defined by Eq. (8).

Now, for structural adhesives, it is often found from experimental tests, for example, Jethwa and Kinloch,[6] Curley *et al.*,[7] Kinloch *et al.*,[12] Azari *et al.*,[26] and Ashcroft and Shaw,[27] that a clearly defined threshold value exists, below which little fatigue crack growth occurs. In this case, the value of the threshold, $\Delta\sqrt{G_{Ithr}}$, is taken to be the experimentally determined value. If this is not the case, then the concepts described in the ASTM standard,[28] which are widely used by the metals community, may be employed. This standard defines a threshold value that, in the previous terminology, may be taken to be the value of $\Delta\sqrt{G_I}$ at a value of da/dN of 10^{-10} m cycle^{-1}. This is termed $\Delta\sqrt{G_{Ith}}$, and hence, by rearrangement of Eq. (6), the value of $\Delta\sqrt{G_{Ithr}}$ is given by

$$\Delta\sqrt{G_{Ithr}} = \Delta\sqrt{G_{Ith}} - \sqrt{\left\{1 - \sqrt{G_{Imax}}/\sqrt{A}\right\}}\left[\frac{10^{-10}}{D}\right]^{1/n} \tag{9}$$

with the experimental data having G with units of Joule per square metre and da/dN with units of metre per cycle.

The literature reveals that for structural adhesive joints, a pronounced threshold region often exists in the typical fatigue plots of log(da/dN) versus log (G_{Imax}). Therefore, a well-defined experimental value of $G_{Ithr.max}$, where $G_{Ithr.max}$ is the maximum value of G_I at the threshold, may be deduced; for example, see later in Figs 1 and 2. Such a well-defined experimental value of the threshold, which may be expressed in terms of $G_{Ithr.max}$, ΔG_{Ithr} or $\Delta\sqrt{G_{Ithr}}$, implies that Eq. (6) will only give a linear representation of the experimentally measured fatigue behaviour if a suitable criterion is imposed. In the present work, therefore, the following criterion has been adopted for considering the validity of the experimental data points to plot via the Hartman–Schijve equation:

$$G_{Imax} > G_{Ithr.max} \tag{10}$$

or, of course, the equivalent inequality in terms of ΔG_{Ithr} or $\Delta\sqrt{G_{Ithr}}$.

Adhesive joints can also undergo fatigue crack growth under Mode II (in-plane shear) loading. In this case, the Mode II form of the Hartman–Schijve equation can be expressed by

†However, it should be recalled that this equation, like all of the equations that are widely used to represent crack growth in metals, is basically empirical.

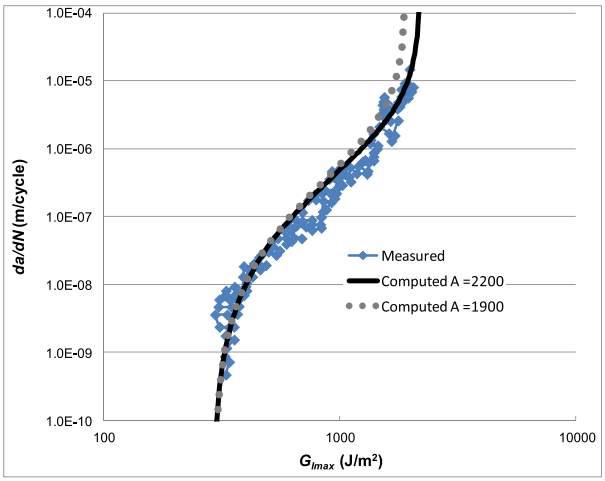

Fig. 2 The measured[6] and computed Mode I fatigue behaviour for a rubber-toughened epoxy-paste adhesive ('XD4600'). (Results from five replicate tests are given. Values of A are in Joule per square metre).

$$\frac{da}{dN} = D\left[\frac{\Delta\sqrt{G_{II}} - \Delta\sqrt{G_{IIthr}}}{\sqrt{\left\{1 - \sqrt{G_{IImax}}/\sqrt{A}\right\}}}\right]^n \qquad (11)$$

where D, n and A are again constants and the subscript '*II*' indicates Mode II loading. (Note: if Mixed-Mode I/II fatigue loading has been applied to the structural adhesive joints, then the subscript '*I/II*' has been employed.)

Considering the parameters in Eqs (6) and (11), then, as explained earlier, the value of $\Delta\sqrt{G_{Ithr}}$ is experimentally measured for those adhesives where a clearly defined threshold value exists, below which little fatigue crack growth occurs. If this is not the case, then it is calculated via Eq. (9). As discussed by Jones,[16] the value of A is best interpreted as a parameter chosen so as to fit the experimentally measured da/dN versus ΔG_I (or G_{Imax}) data. To do this, log da/dN is first plotted against log $\left[\frac{\Delta\sqrt{G_I} - \Delta\sqrt{G_{Ithr}}}{\sqrt{\left\{1 - \sqrt{G_{Imax}}/\sqrt{A}\right\}}}\right]$, taking A to be the quasi-static value of the fracture energy, G_c, or any reasonable first estimate. The value of A is then chosen by refining its value such that these experimental data, for each data set, lie, approximately, on a single straight line. The values of D and n are then obtained via using a best fit power-law representation of the experimental data of log(da/dN) against log $\left[\frac{\Delta\sqrt{G_I} - \Delta\sqrt{G_{Ithr}}}{\sqrt{\left\{1 - \sqrt{G_{Imax}}/\sqrt{A}\right\}}}\right]$. (The same procedure is being adopted for the other modes of loading, as appropriate.)

The detailed aims of the present paper are to explore, for the first time, the validity of the Hartman–Schijve approach, as embodied in Eqs (6) and (11), when applied to cyclic-fatigue crack growth in structural adhesive joints. There is a special emphasis on exploring in detail, for a given adhesive, several important aspects of the Hartman–Schijve approach, namely whether

- A 'master' linear representation for the fatigue data may be obtained when the experimentally measured data are conveniently plotted according to an equation of the form of Eq. (6) or (11).
- The slope, n, of this 'master' linear relationship has a relatively low value, ideally of the order of about two. Because this would imply that the Hartman–Schijve equation is suitable for enabling engineers to allow for some (limited) fatigue crack growth to be permitted when designing with structural adhesives, as opposed to imposing the rigidly implemented 'no crack-growth' criterion.
- The Hartman–Schijve equation may account for R-ratio and test temperature effects and will also readily account for the degree of variability, and hence scatter, typically observed in cyclic-fatigue tests on structural adhesives.
- Having ascertained the constants in the Hartman–Schijve equation [i.e. Eq. (6) or (11)], the complete curve for the experimentally measured results (i.e. typically of the form da/dN versus G_{max}, or ΔG) may be accurately computed.
- The results from Mode I, Mode II and Mixed-Mode I/II types of fatigue loading may all be conveniently modelled via Eq. (6) or (11), as appropriate.

RESULTS AND DISCUSSION

Firstly, fatigue crack growth for structural adhesive joints obtained using LEFM, and typically employing Mode I test specimens based upon the double-cantilever beam (DCB) or tapered DCB (TDCB) test specimens,[4] will be considered. Mixed-Mode I/II test data on the fatigue crack growth for structural adhesive joints will then be reviewed, and then, Mode II fatigue crack growth will be considered. Finally, a comparison of the fatigue behaviour of a given structural adhesive obtained using both Mode I and Mode II fatigue loadings will be undertaken. Wherever possible, the effects of test conditions, such as the R-ratio, test temperature and mode of loading, and the degree of scatter seen in the experimental results will be examined with respect to establishing the validity, and usefulness, of the Hartman–Schijve equation.

Mode I fatigue crack growth: basic approach

Fatigue crack-growth data may be found in the literature[6] for a rubber-toughened epoxy-paste adhesive (Dow Automotive, USA, 'XD4600'), which is a typical

structural adhesive. In the study of Jethwa and Kinloch,[6] LEFM TDCB tests were conducted at $R = 0.5$, 23 ± 1 °C, and a relative humidity of 55 ± 5%RH. A plot of the resultant log *da/dN* versus log G_{Imax} data is shown in Fig. 2. For convenience, the experimental data given in Fig. 2 are shown replotted in Fig. 3 according to the Hartman–Schijve approach embodied in Eq. (6). Hence, log *da/dN* is plotted against log $\left[\frac{\Delta\sqrt{G_I} - \Delta\sqrt{G_{Ithr}}}{\sqrt{\left\{1 - \sqrt{G_{Imax}}/\sqrt{A}\right\}}}\right]$, and the values of the various parameters employed are given in Table 1. The plot in Fig. 3 is indeed linear with a low degree of scatter, as revealed by the relatively high value of the correlation coefficient that has been deduced. This linear plot has a slope, *n*, of about two. This value is relatively low compared with the value of the exponent for the linear region in Fig. 2, which is about four in value.

Equation (6), together with the values of the parameters given in Table 1, can now be used to compute the full experimental fatigue curve of *da/dN* versus the value of G_{Imax}. This computed relationship is also shown in Fig. 2, and, as maybe seen, there is excellent agreement between the experimental data and the computed curve from the Hartman–Schijve approach. Thus, the cyclic-fatigue behaviour under Mode I loading of the 'XD4600' structural adhesive may indeed be very well represented using the Hartman–Schijve equation. Whereas the computed curve discussed earlier and shown in Fig. 2 used a value of $A = 2200\,\mathrm{J\,m^{-2}}$, to illustrate how to refine the value of *A*, then Fig. 2 also presents the computed relationship using the value of $A = 1900\,\mathrm{J\,m^{-2}}$. Here, it can be seen that the primary effect of changes in *A* is associated with Region III, that is, the region of rapid growth. As such, the value of *A* can be 'fine tuned' so as to ensure that the equation best represents the data in this region.

Table 1 Values of the parameters employed in the Hartman–Schijve Eq. (6) for Mode I crack growth in the 'XD4600' adhesive

D (m cycle^{-1})	n	A (J m^{-2})	$\Delta\sqrt{G_{Ithr}}$ ($\sqrt{(\mathrm{J\,m^{-2}})}$)
2.48×10^{-9}	2.07	2200	8.5[a]

[a]The experimentally determined value from Jethwa and Kinloch.[6]

Considerations of the experimental variability

Fatigue crack-growth data for a rubber-toughened epoxy-film adhesive (Hysol Dexter, USA, 'EA9628') is given by Kinloch *et al.*,[12] who presented the results of DCB tests at $R = 0.5$, 23 ± 1 °C, and a relative humidity of 55 ± 5%RH. A plot of the experimentally obtained log *da/dN* versus log G_{Imax} data is given in Fig. 4. Comparing Figs 2 and 4, it may be seen that there is somewhat more variability, and hence scatter, in the experimental results from these replicate tests presented in Fig. 4 than for the previous results shown in Fig. 2.

The experimental data given in Fig. 4 are shown replotted in Fig. 5 according to Eq. (6). In this figure, log *da/dN* is plotted against log $\left[\frac{\Delta\sqrt{G_I} - \Delta\sqrt{G_{Ithr}}}{\sqrt{\left\{1 - \sqrt{G_{Imax}}/\sqrt{A}\right\}}}\right]$, and the values of the various parameters employed are given in Table 2. It should be noted that the values for each of the constants *D*, *n* and *A* in Eq. (6) have, for convenience, been taken to be the same value for all the five replicate tests. However, the values of $\Delta\sqrt{G_{Ithr}}$ have been measured from the experimental data for the individual replicate tests. Several noteworthy points emerge from the results

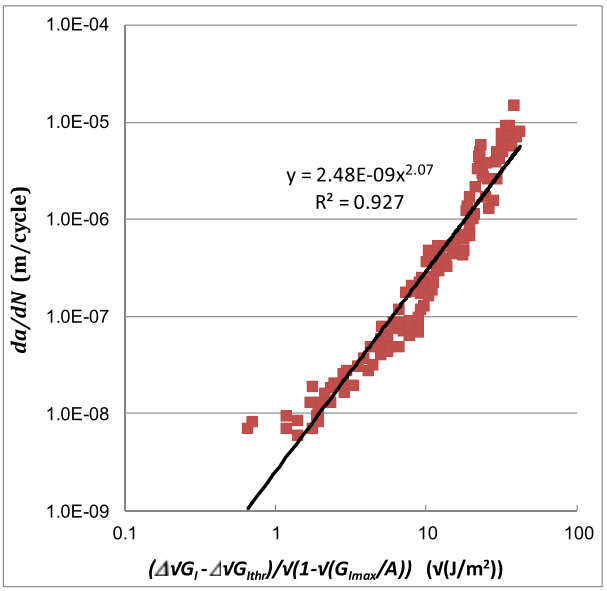

Fig. 3 The Hartman–Schijve representation of the Mode I fatigue behaviour for a rubber-toughened epoxy-paste adhesive ('XD4600').

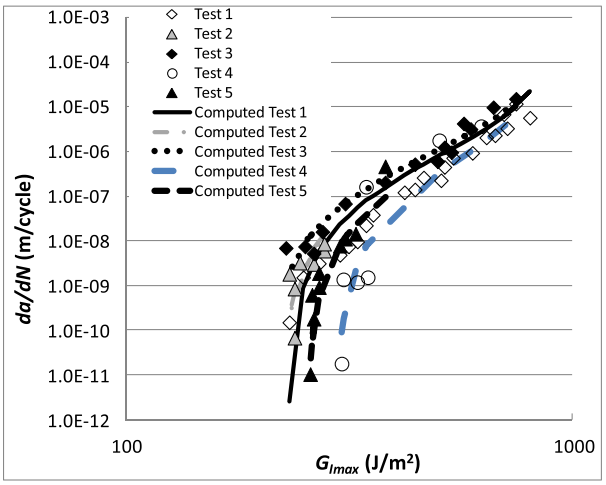

Fig. 4 The measured[12] and computed curves for the Mode I fatigue behaviour for a rubber-toughened epoxy-film adhesive ('EA9628').

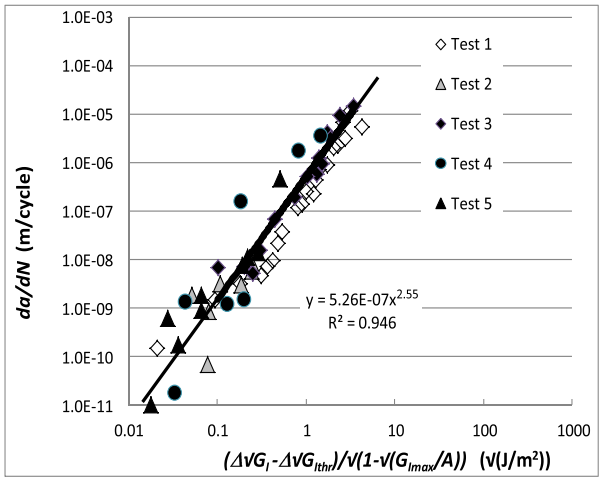

Fig. 5 The Hartman–Schijve representation of the Mode I fatigue behaviour for a rubber-toughened epoxy-film adhesive ('EA9628').

Table 2 Values of the constants employed in the Hartman–Schijve Eq. (6) for Mode I crack growth in the 'EA9628' adhesive

Test	D (m cycle^{-1})	n	A (J m^{-2})	$\Delta\sqrt{G_{Itbr}}$ ($\sqrt{}$(J m^{-2}))
1	5.26×10^{-7}	2.55	900	7.53[a]
2	5.26×10^{-7}	2.55	900	7.42[a]
3	5.26×10^{-7}	2.55	900	7.16[a]
4	5.26×10^{-7}	2.55	900	8.58[a]
5	5.26×10^{-7}	2.55	900	7.97[a]

[a]The experimentally determined values from Kinloch *et al.*[12]

shown in Fig. 5. Firstly, the plot is indeed linear and gives a unique 'master' linear relationship, with a low degree of scatter, for all the replicate tests. Thus, the variability seen in the replicate tests, as shown in Fig. 4, has indeed been accounted for by using the Hartman–Schijve equation, employing the appropriate experimentally measured values of $\Delta\sqrt{G_{Itbr}}$; see Table 2. Secondly, this 'master' linear relationship has a slope, n, of 2.55, which is relatively low in comparison with the value of the exponent of about seven to eight for the linear region of the data shown in Fig. 4.

Equation (6), together with the values of the parameters given in Table 2, can now be used to compute the full experimental fatigue curves of da/dN versus the value of G_{Imax}, for each of the replicate tests. These computed relationships, for each replicate, are also shown plotted in Fig. 4, and, as maybe seen, there is excellent agreement between the experimental data and the computed representation. Thus, the Mode I cyclic-fatigue behaviour of the 'EA9628' structural adhesive may indeed be very well and conveniently represented using the Hartman–Schijve equation. Of special note is the observation that the variability in the fatigue results may be taken into account by this approach from employing the experimentally measured values of $\Delta\sqrt{G_{Itbr}}$, which do vary somewhat for the replicate test specimens, as shown in Table 2.

The effect of *R*-ratio

The effects of changing the R-ratio on the fatigue behaviour have been reported[9] for a structural adhesive based upon a rubber-toughened acrylic adhesive (Loctite, Eire, 'Multibond 330'). In this work, room temperature DCB tests were undertaken at a frequency of 10 Hz and an R-ratio of either 0.1 or 0.4. The associated experimental results are shown in Fig. 6, which reveals a definite R-ratio effect with a higher R-ratio leading to an inferior fatigue behaviour.

The experimental data given in Fig. 6 are shown replotted in Fig. 7 according to Eq. (6), where log da/dN is plotted against log $\left[\frac{\Delta\sqrt{G_I}-\Delta\sqrt{G_{Ithr}}}{\sqrt{\left\{1-\sqrt{G_{Imax}}/\sqrt{A}\right\}}}\right]$ and the values of the various parameters employed are given in Table 3. In accord with the previous analysis, it should be noted that the values for each of the constants D, n and A have, for convenience, been taken to be the same value for both values of the R-ratio. However, the values of $\Delta\sqrt{G_{Itbr}}$ have been calculated from the experiments undertaken for each individual R-ratio using Eq. (9). Figure 7 again reveals a linear unique 'master' linear relationship, with a low degree of scatter, for these two R-ratios. Thus, the fatigue behaviour of the 'Multibond 330' structural acrylic adhesive may indeed be very well represented using Eq. (6), and the effects of the R-ratio may also be taken into account. Further, this 'master' linear relationship has a slope, n, of 1.75, which is relatively low in value compared with the value of about four for the linear region for the measured data shown in Fig. 6.

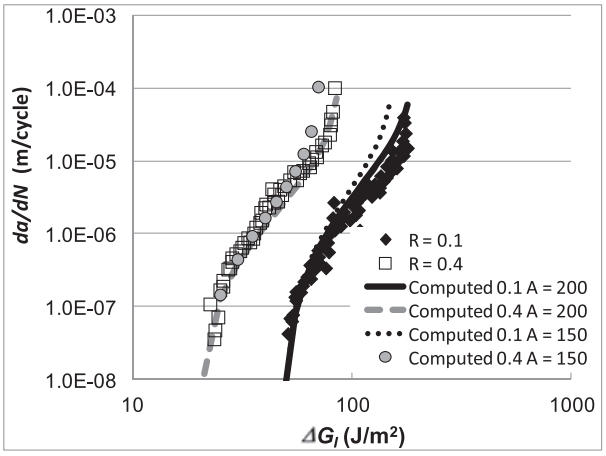

Fig. 6 The measured[9] and computed curves for the Mode I fatigue behaviour for a rubber-toughened acrylic adhesive ('Multibond 330'; values of A in Joule per square metre).

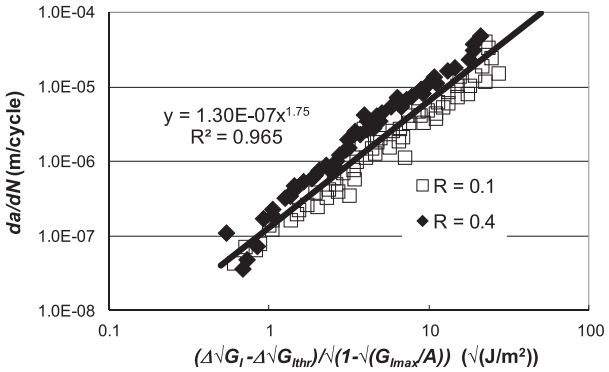

Fig. 7 The Hartman–Schijve representation of the Mode I fatigue behaviour for a rubber-toughened acrylic adhesive ('Multibond 330').

Table 3 Values of the parameters employed in the Hartman–Schijve Eq. (6) for Mode I crack growth in the 'Multibond 330' adhesive

R-ratio	D (m cycle^{-1})	n	A (J m^{-2})	$\Delta\sqrt{G_{Ithr}}$ ($\sqrt{}$(J m^{-2}))
$R=0.1$	1.30×10^{-7}	1.75	200	6.9[a]
$R=0.4$	1.30×10^{-7}	1.75	200	4.4[a]

[a]The experimentally determined values from Pirondi and Nicoletto.[9]

Equation (6), together with the values of the parameters given in Table 3, can now be used to compute the full of da/dN versus ΔG_I relationship for each of the two different R-ratios. Figure 6 reveals that in each case, there is excellent agreement between the experimental and the computed curves. Whereas the computed curves discussed earlier and shown in Fig. 6 used a value of $A=200\,\mathrm{J\,m^{-2}}$, to further illustrate how to refine the value of A, then Fig. 6 also presents the computed relationship using the value of $A=150\,\mathrm{J\,m^{-2}}$. Here again, it can be seen that the primary effect of changes in A is associated with Region III, that is, the region of rapid growth. As such, this example further illustrates the fact that the value of A can be 'fine tuned' so as to ensure that the Hartman–Shrive equation best represents the data in this region.

Mixed-Mode I/II fatigue crack growth

The previous studies have clearly demonstrated the success of employing the Hartman–Schijve approach, as embodied in Eq. (6), to analyse the cyclic-fatigue crack growth under Mode I loading in several types of structural adhesives. The results have also revealed the ability of the Hartman–Schijve equation to yield a unique 'master' linear relationship, which may account for the degree of scatter that is often seen in such fatigue tests and the effects of changing the R-ratio.

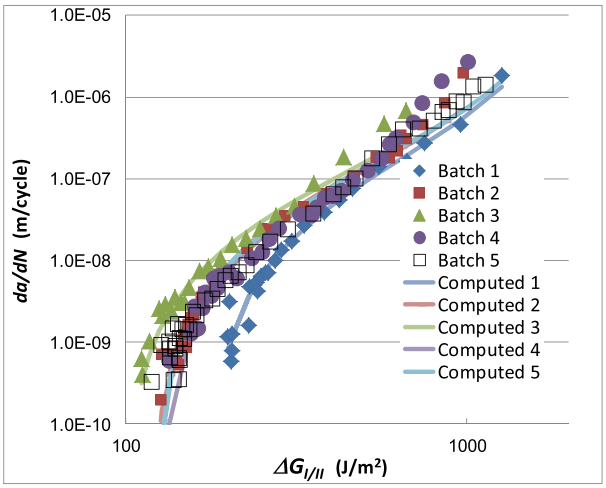

Fig. 8 The measured[26] and computed curves for the Mixed-Mode I/II fatigue behaviour for a toughened-epoxy adhesive.

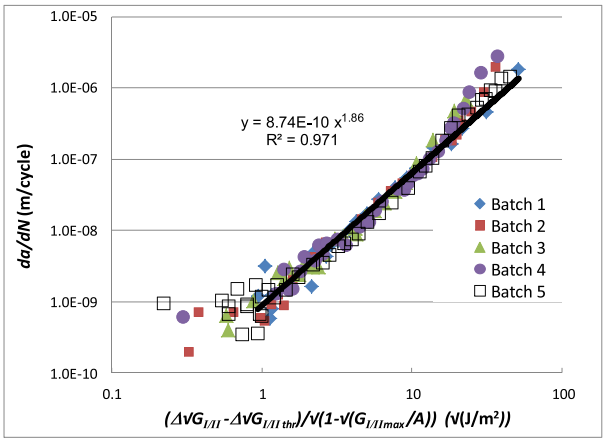

Fig. 9 The Hartman–Schijve representation of the Mode I/II fatigue behaviour for a toughened-epoxy adhesive.

A study of the fatigue behaviour of structural adhesive joints when subjected to Mixed-Mode I/II loading is now undertaken. Such experimental results have been reported[26] for a toughened-epoxy structural adhesive tested at room temperature, a frequency of 20 Hz and an $R=0.1$. In this work, asymmetric-DCB tests were undertaken, and Fig. 8 shows the experimental results obtained in a plot of log da/dN versus log $\Delta G_{I/II}$. Again, it may be seen that these replicate tests give some degree of variability, and hence scatter, in the measured results.

The experimental data given in Fig. 8 are shown replotted in Fig. 9 according to the Hartman–Schijve approach embodied in Eq. (11). Hence, log da/dN is plotted against log $\left[\frac{\Delta\sqrt{G_{I/II}}-\Delta\sqrt{G_{I/IIthr}}}{\sqrt{\{1-\sqrt{G_{I/IImax}}/\sqrt{A}\}}}\right]$, and the values of the various parameters employed are given in Table 4. It should be noted that the values for each of the constants D, n and A in Eq. (11) have again been taken to be the same value

Table 4 Values of the parameters employed in the Hartman–Schijve Eq. (11) for Mixed-Mode I/II crack growth in the toughened-epoxy adhesive

Batch	D (m cycle^{-1})	n	A (J m^{-2})	$\Delta\sqrt{G_{I/IIthr}}$ ($\sqrt{(}$J m^{-2}))
1	8.74×10^{-10}	1.86	1800	12.0
2	8.74×10^{-10}	1.86	1800	9.9
3	8.74×10^{-10}	1.86	1800	9.0
4	8.74×10^{-10}	1.86	1800	10.0
5	8.74×10^{-10}	1.86	1800	10.0

for all the five replicate tests, whilst the values of $\Delta\sqrt{G_{I/IIthr}}$ have been calculated for the individual replicate experiments. Several noteworthy points emerge from the results shown in Fig. 9. Firstly, the plot is indeed linear and gives a unique 'master' relationship, with a far lower degree of scatter than Fig. 8. Thus, the variability seen in the replicate tests, as shown in Fig. 8, has indeed been accounted for by using Eq. (11) with the calculated values of $\Delta\sqrt{G_{I/IIthr}}$. Secondly, this 'master' linear relationship has a slope, n, of about two, which is relatively low in comparison with the value of about four for the linear region for the measured data shown in Fig. 8.

Equation (11), together with the values of the parameters given in Table 4, can now be used to compute the da/dN versus $\Delta G_{I/II}$ relationship for each replicate tests; see Fig. 8. These computed relationships for each replicate test are also shown plotted in Fig. 8 where we again see an excellent agreement between the experimental and the computed curves. Thus, the Mode I/II cyclic-fatigue behaviour of this toughened-epoxy structural adhesive may indeed be represented using Eq. (11), and the degree of variability observed in the measured fatigue results may also be taken into account.

Mode II fatigue crack growth

The cyclic-fatigue behaviour under Mode II loading of two structural epoxy-film adhesives (i.e. FM300K and FM300 from Cytec, USA) that are used in the manufacture and repair of the composite structure on the 'F/A-18' aircraft has been reported by Russell.[29] The fatigue tests were conducted under Mode II loading using the end-loaded split test specimen. The frequency of the test was varied from 0.1 to 4 Hz, and no significant of effect of the test frequencies was observed. The other experimental variables studied included the R-ratio, with values of $R=0$ and $R=-1$ being employed, and three test temperatures were chosen, namely −50, 100 and 20 °C.

Figures 10 and 11 present the Mode II fatigue results as a plot log da/dN versus log ΔG_{II} curves for the epoxy-film adhesives 'FM300K' and 'FM300', respectively. The

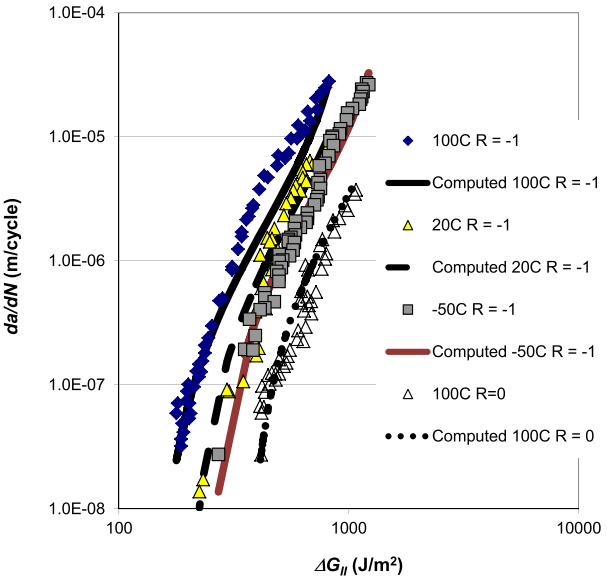

Fig. 10 The measured[29] and computed curves for the Mode II fatigue behaviour for the epoxy-film adhesive 'FM300K'.

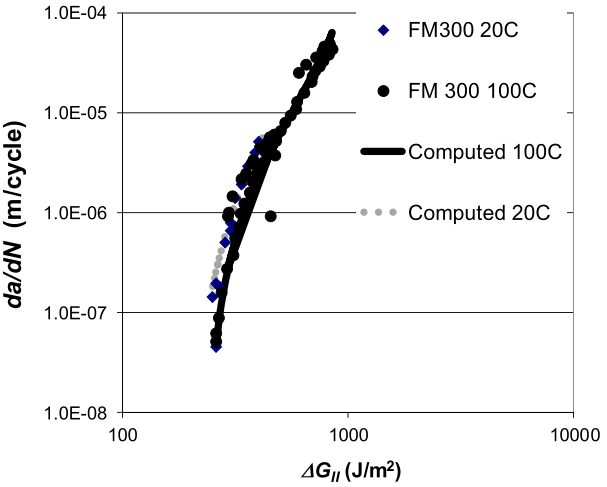

Fig. 11 The measured[29] and computed curves for the Mode II fatigue behaviour for the epoxy adhesive 'FM300'; all tests are for $R=-1$.

experimental Mode II data given in these figures are replotted in Figs 12 and 13, respectively, according to Eq. (11) where log da/dN is plotted against log $\left[\frac{\Delta\sqrt{G_{II}}-\Delta\sqrt{G_{IIthr}}}{\sqrt{\left\{1-\sqrt{G_{IImax}}/\sqrt{A}\right\}}}\right]$ and the values of the various parameters employed are given in Tables 5 and 6. It should be noted that, in each case, the values for the constants D and n in Eq. (11) have been taken to be the same for all the tests. The values of A and $\Delta\sqrt{G_{IIthr}}$ have been calculated, as described earlier, from the individual experimental data. Figures 12 and 13 reveal

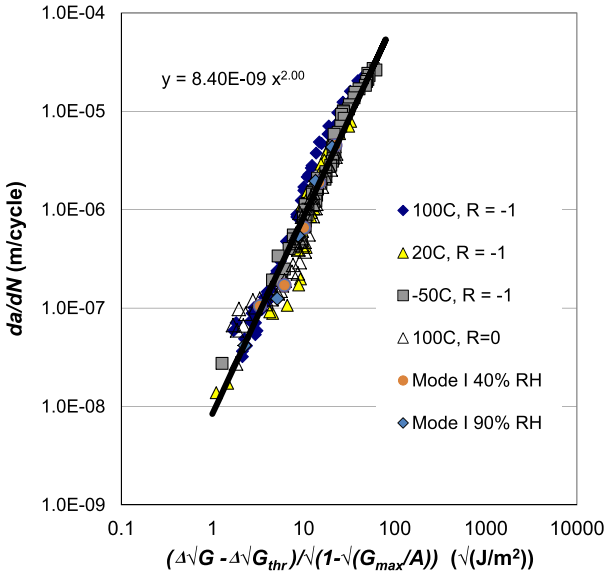

Fig. 12 The Hartman–Schijve representation of the Mode II and Mode I fatigue behaviours for the epoxy-film adhesive 'FM300K'.

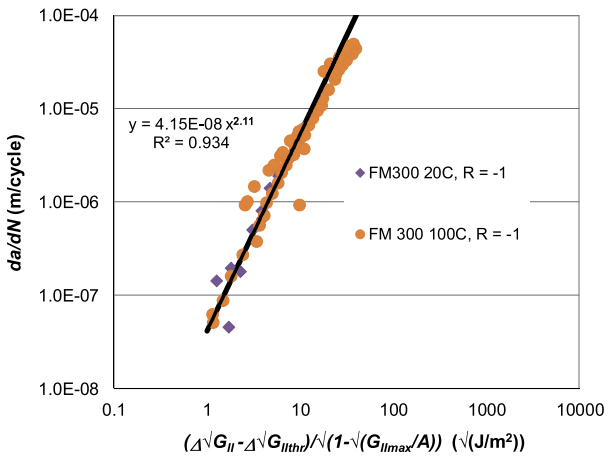

Fig. 13 The Hartman–Schijve representation of the Mode II fatigue behaviour for the epoxy adhesive 'FM300'.

that, in both cases, the various *R*-ratio and temperature-dependent curves essentially collapse onto a single 'master' linear plot when Eq. (11) is employed to represent the fatigue data.

Thus, in each case, the Mode II cyclic-fatigue behaviour of the structural adhesives FM300K and FM300 may be represented using the Eq. (11) and, indeed, in Fig. 12, for example, the effects of the *R*-ratio and test temperature collapse onto a single 'master' linear plot with a correlation coefficient of 0.976.

Equation (11), together with the values of the parameters given in Tables 5 and 6, was then used to compute the full experimental fatigue *da/dN* versus the value of ΔG_{II} relationship for these two epoxy adhesives. These computed relationships for each test temperature are also shown plotted in Figs 10 and 11, and, as maybe seen, there is excellent agreement between the experimental data and the computed relationships. Thus, the Mode II cyclic-fatigue behaviour of both the 'FM300K' and 'FM300' structural adhesives may indeed be represented using the Hartman–Schijve approach. The effects of the *R*-ratio and test temperature are seen to collapse onto a single 'master' linear plot, which exhibits a low degree of scatter, for each adhesive. These 'master' relationships, which capture the effects of both the *R*-ratio and the test temperature under Mode II loading, have a slope, *n*, of about two; see Figs 12 and 13. This value of the exponent is relatively low in comparison with the values of about four to six for the linear regions for the measured data shown in Figs 10 and 11.

The correlation of Mode I and Mode II fatigue crack growth

It is of interest that Mode I fatigue crack-growth data for the epoxy-film adhesive 'FM300K', for which the Mode II fatigue results are given earlier, obtained using TDCB tests, have been reported by Ripling *et al.*[30] The

Table 5 Values of the parameters employed in the Hartman–Schijve Eq. (11) for Mode II crack growth in the 'FM300K' adhesive

Test	D (m cycle^{-1})	n	A (J m^{-2})	$\Delta\sqrt{G_{IIthr}}$ ($\sqrt{}$(J m^{-2}))
100 °C and $R=-1$	8.40×10^{-9}	2.00	975	12.5
20 °C and $R=-1$	8.40×10^{-9}	2.00	1200	14.1
−50 °C and $R=-1$	8.40×10^{-9}	2.00	1500	15.5
100 °C and $R=0$	8.40×10^{-9}	2.00	2700	10.0

Table 6 Values of the parameters employed in the Hartman–Schijve Eq. (11) for Mode II crack growth in the 'FM300' adhesive

Test	D (m cycle^{-1})	n	A (J m^{-2})	$\Delta\sqrt{G_{IIthr}}$ ($\sqrt{}$ (J m^{-2}))
100 °C and $R=-1$	4.15×10^{-8}	2.11	1100	15.3
20 °C and $R=-1$	4.15×10^{-8}	2.11	755	15.0

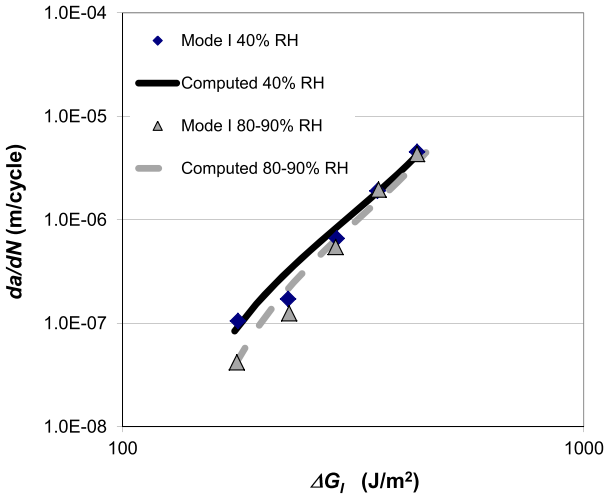

Fig. 14 The measured[30] and computed Mode I fatigue behaviour for the adhesive 'FM300K'.

Mode I tests were conducted at 20 °C and in both a 40%RH and a 90%RH environment. The measured *da/dN* versus ΔG_I plots[30] are shown in Fig. 14, together with the computed relationships using Eq. (6). The values of the parameters employed in Eq. (6) are given in Table 7. It should be noted that the values of the constants D and n used for these Mode I tests were taken to be the same as those used for the Mode II tests; see Table 5. The values of A and $\Delta\sqrt{G_{Ithr}}$ were calculated, as described earlier, with the value of A being a constant for these Mode I tests. From Fig. 14, it may be seen that there is excellent agreement between the experimental data and the Mode I curves computed using Eq. (6).

The experimental Mode I data given in Fig. 14 are shown replotted in Fig. 12 according to Eq. (6). Hence, for these Mode I results, log (*da/dN*) is plotted against $\log\left[\frac{\Delta\sqrt{G_I}-\Delta\sqrt{G_{Ithr}}}{\sqrt{\left\{1-\sqrt{G_{Imax}}/\sqrt{A}\right\}}}\right]$, and the values of the various parameters employed are given in Table 7. The plot in Fig. 12 is linear, and it should be noted that this linear relationship is identical to that previously obtained to describe the Mode II fatigue data. Thus, the Hartman–Schijve approach appears to yield a convenient 'master' linear relationship that describes both the Mode I and the Mode II fatigue behaviours for the 'FM300K' adhesive. Further, this 'master' relationship has a slope, n, of two, which is relatively low in comparison with the values of between six and four for the linear regions for the measured data shown in Figs 10 and 14, respectively. Comparing the *da/dN* versus ΔG plots for Mode II and Mode I fatigue loadings, see Figs 10 and 14, respectively, then clearly at 20 °C, the fatigue behaviour of the epoxy-film adhesive 'FM300K' is significantly superior under Mode II loading. This is reflected in the values of the terms A and $\Delta\sqrt{G_{thr}}$, as used in the Hartman–Schijve equations, being significantly higher for tests conducted under Mode II fatigue loading compared with under Mode I fatigue loading; see Tables 5 and 7.

CONCLUSIONS

The present paper has shown, for the first time, the exciting potential for the Hartman–Schijve approach to unify many aspects of the cyclic-fatigue crack-growth behaviour that have been observed in structural adhesive joints. The Hartman–Schijve approach has, for example, revealed several noteworthy features for a wide range of structural adhesives:

- A 'master' linear representation has been observed for each adhesive studied when such data are replotted according to the Hartman–Schijve Eq. (6) or (11).
- The slope, n, of this 'master' linear relationship has a relatively low value of about two. As discussed earlier, this will greatly assist a designer to allow for some fatigue crack growth to occur but still provide a safe life for the adhesively bonded structure.
- The variability, and hence the scatter, which was sometimes observed in the typical log *da/dN* versus log ΔG_I (or G_{Imax}) plots from testing replicate specimens, has been captured by varying only the fatigue threshold term, $\Delta\sqrt{G_{Ithr}}$, in the Hartman–Schijve equation, with the value of $\Delta\sqrt{G_{Ithr}}$ being ascertained either via direct measurement or as calculated from Eq. (9). Indeed, the degree of scatter associated with the Hartman–Schijve 'master' linear relationships was always found to be relatively low, as observed by the relatively high values of the correlation coefficients that were deduced.
- Having ascertained the constants in the Hartman–Schijve equation [i.e. Eq. (6) or (11)], it has been shown that the complete curve for the experimentally measured

Table 7 Values of the parameters employed in the Hartman–Schijve Eq. (6) for Mode I crack growth in the 'FM300K' adhesive

Test RH	D (m cycle^{-1})	n	A (J m^{-2})	$\Delta\sqrt{G_{Ithr}}$ ($\sqrt{}$(J m^{-2}))
40% RH	8.40×10^{-9}	2.00	630	9.8
80–90% RH	8.40×10^{-9}	2.00	630	10.5

results (i.e. typically of the form da/dN versus G_{max} or ΔG) could be computed with a relatively high degree of accuracy.

- The Hartman–Schijve approach may account for both R-ratio and test temperature effects, again yielding a unique 'master' linear relationship, which captures these effects.
- The Hartman–Schijve approach was found to be applicable to Mode I, Mode II and Mixed-Mode I/II types of fatigue loading. Indeed, it has been demonstrated that both the Mode I and the Mode II fatigue behaviours for an adhesive may be conveniently described by a single, unique, 'master' linear relationship via the Hartman–Schijve approach.

The previous conclusions demonstrate that the Hartman–Schijve approach can indeed be used to represent the fatigue crack-growth results that have been reported in the literature on tests involving 'long cracks' in structural adhesive joints. Thus, in future work, we intend to extend these studies to 'short cracks' and to explore the use of the Hartman–Schijve approach for designing and predicting the lifetime of structural adhesive joints subjected to cyclic fatigue.

REFERENCES

1 Miedlar, P. C., Berens, A. P., Gunderson, A. and Gallagher, J. P. (2003) Analysis and Support Initiative for Structural Technology (ASIST). AFRL-VA-WP-TR-2003-3002, Ohio, USA.

2 Pascoe, J. A., Alderliesten, R. C. and Benedictus, R. (2013) Methods for the prediction of fatigue delamination growth in composites and adhesive bonds – a critical review. *Eng. Fract. Mech.*, **112-113**, 72–96.

3 Azari, S., Jhin, G., Papini, M. and Spelt, J. K. (2014) Fatigue threshold and crack growth rate of adhesively bonded joints as a function of load/displacement ratio. *Compos.*, **57**, 59–66.

4 ISO. (2009) Adhesives – Determination of the Mode I Adhesive Fracture Energy G_{Ic} of Structural Adhesive Joints Using Double Cantilever Beam and Tapered Double Beam Specimens. ISO 25217, Geneva, Switzerland.

5 Ripling, E. J., Mostovoy, S. and Patrick, R. L. (1963) Application of fracture mechanics to adhesive joints. *ASTM STP*, **360**, 5–19.

6 Jethwa, J. K. and Kinloch, A. J. (1997) The fatigue and durability behaviour of automotive adhesives. Part 1: fracture mechanics tests. *J. Adhes.*, **61**, 71–95.

7 Curley, A. J., Hadavinia, H., Kinloch, A. J. and Taylor, A. C. (2000) Predicting the service-life of adhesively-bonded joints. *Int. J. Fract.*, **103**, 41–70.

8 Mall, S., Ramamurthy, G. and Rezaizdeh, M. A. (1987) Stress ratio effect on cyclic debonding in adhesively bonded joints. *Compos. Struct.*, **8**, 31–45.

9 Pirondi, A. and Nicoletto, G. (2004) Fatigue crack growth in bonded DCB specimens. *Eng. Fract. Mech.*, **71**, 859–871.

10 Martin, R. H. and Murri, G. B. (1990) Characterization of Mode I and Mode II delamination growth and thresholds in AS4/PEEK composites. *ASTM STP*, **1059**, 251–270.

11 Jones, R., Pitt, S., Brunner, A. J. and Hui, D. (2012) Application of the Hartman–Schijve equation to represent Mode I and Mode II fatigue delamination growth in composites. *Compos. Struct.*, **94**, 1343–1351.

12 Kinloch, A. J., Little, M. S. G. and Watts, J. F. (2000) The role of the interphase in the environmental failure of adhesive joints. *Acta Mater.*, **48**, 4543–4553.

13 Rouchon, J. (2009) Fatigue and damage tolerance evaluation of structures: the composite materials response, 22nd Plantema Memorial Lecture, 25th Symposium of the International Committee on Aeronautical Fatigue, 27 May 2009, Rotterdam, The Netherlands. (Also published as NLR-TP-2009-221).

14 Jones, R., Stelzer, S. and Brunner, A. J. (2014) Mode I, II and Mixed Mode I/II delamination growth in composites. *Compos. Struct.*, **110**, 317–324.

15 Federal Aviation Authority. (2009) Airworthiness Advisory Circular No: 20-107B. *Composite Aircraft Structure*, 09/08/2009.

16 Jones, R. (2014) Fatigue crack growth and damage tolerance. *Fatig. Fract. Eng. Mater. Struct.*, **37**, 463–483.

17 Hartman, A. and Schijve, J. (1970) The effects of environment and load frequency on the crack propagation law for macro fatigue crack growth in aluminium alloys. *Eng. Fract. Mech.*, **1**, 615–631.

18 Molent, L., Barter, S. A. and Wanhill, R. J. H. (2011) The lead crack fatigue lifing framework. *Int. J. Fatig.*, **33**, 323–331.

19 Wanhill, R. J. H. (2009) Characteristic Stress Intensity Factor Correlations of Fatigue Crack Growth in High Strength Alloys: Reviews and Completion of NLR Investigations 1985–1990. NLR-TP-2009-256.

20 Molent, L. (2014) A review of equivalent pre-crack sizes in aluminium alloy 7050-T7451, *Fatig. Fract. Eng. Mater. Struct.*. DOI: 10.1111/ffe.12214

21 Wang, S. S., Mandell, J. F. and McGarry, F. J. (1978) Analysis of crack tip stress-field in DCB adhesive fracture specimens. *Int. J. Fract.*, **14**, 39–58.

22 Tvergaard, V. and Hutchinson, J. W. (1993) The influence of plasticity on mixed mode interface toughness. *J. Mech. Phys. Solid*, **41**, 1119–1135.

23 Kinloch, A. J. (1997) Adhesives in engineering. *Proc. IME*, **211**, 307–334.

24 Rans, C., Alderliesten, R. C. and Benedictus, R. (2011) Misinterpreting the results: how similitude can improve our understanding of fatigue delamination growth. *Compos. Sci. Tech.*, **71**, 230–238.

25 Knott, J. F. (1984) Fatigue Crack Growth. 30 Years of Progress (Edited by R. A. Smith), Pergamon Press, Oxford, UK, pp. 31–52.

26 Azari, S., Papini, M., Schroeder, J. and Spelt, J. K. (2010) Fatigue threshold behaviour of adhesive joints. *Int. J. Adhes. Adhes.*, **30**, 145–159.

27 Ashcroft, I. and Shaw, S. J. (2002) Mode I fracture of epoxy bonded composite joints 2. Fatigue loading. *Int. J. Adhes. Adhes.*, **22**, 151–167.

28 ASTM. (2013) Measurement of Fatigue Crack Growth Rates. ASTM E647-13, USA.

29 Russell, A. J. (1988) A Damage Tolerance Assessment of Bonded Repairs to CF-18 Composite Components. Part I: Adhesive Properties. Canadian Department of National Defence, Defence Research Centre Establishment Pacific, Research and Development Branch, DREP Technical Memorandum-88-25, Canada.

30 Ripling, E. J., Crosley, P. B. and Johnson, W. S. (1988) A comparison of pure Mode I and Mixed-Mode I-III cracking of an adhesive containing an open knit cloth carrier. *ASTM STP*, **981**, 163–182.